13TH CANADIAN MASONRY SYMPOSIUM
HALIFAX, CANADA
JUNE 4TH – JUNE 7TH 2017

TESTING AND FINITE ELEMENT MODELLING OF CONCRETE BLOCK MASONRY IN COMPRESSION

Isfeld, Andrea[1]; Rizaee, Samira[2]; Hagel, Mark[3]; Kaheh, Pedram[4] and Shrive, Nigel[5]

ABSTRACT

The specified concrete block masonry prism strengths for concrete blocks prisms in Table 4 of the CSA-S304-2014 have been shown to be conservative when compared with the blocks available in Alberta. The conservative values in this table, commonly used by designers as an alternative to testing, are becoming obstacles for concrete masonry construction in Alberta. A study was conducted on hollow and fully grouted three course high concrete block prisms constructed using concrete blocks with nominal strengths of 10, 15, 20, and 30 MPa, Type S mortar and coarse grout. Concrete masonry units were tested in compression and their specified strengths determined following the requirements of CSA-S304-2014. Linear relationships were drawn between the actual compressive strength of concrete blocks and the prisms to provide alternative values for the nominal strengths. The laboratory results were also compared to the results of finite element models created in Abaqus for 2, 3, 4 and 5-course prisms. The Abaqus models used the detailed micro-modelling approach and applied a displacement to a steel plate contacting the top of each prism. The results indicate the reduction factors required by the CSA-S304-2014 account sufficiently for the non-homogenous nature of masonry and geometric effects, suggesting 2-course prism testing could be used as the standard test for strength as is required in ASTM C1314.

KEYWORDS: *masonry prism testing, compressive strength, finite element modelling, Canadian masonry standard*

[1] Postdoctoral Scholar, Department of Civil Engineering, Schulich School of Engineering, 2500 University Drive NW, AB, Canada, Canada, acisfeld@ucalgary.ca
[2] Research Assistant, Department of Civil Engineering, Schulich School of Engineering, 2500 University Drive NW, AB, Canada, srizaee@ucalgary.ca
[3] Executive Director, Alberta Masonry Council, P.O.Box 44023, RPO Garside, Edmonton, AB, Canada, markhagel@albertamasonrycouncil.ca
[4] PhD. Candidate, Department of Civil Engineering, Schulich School of Engineering, 2500 University Drive NW, AB, Canada, pkaheh@ucalgary.ca
[5] Professor, Department of Civil Engineering, Schulich School of Engineering, 2500 University Drive NW, AB, Canada, ngshrive@ucalgary.ca

INTRODUCTION

Specified concrete block masonry strengths are listed in Table 4 of CSA-S304-2014, with the option for other values to be used based on test results. The values in Table 4 have largely been in use since 1984 when changes were implemented to base the compressive strength on the mortar bedded area rather than the net cross sectional area [1]. Testing of concrete block, as outlined in Annex D of CSA-S304-2014, requires five course prisms with correction factors applied for prisms with lower aspect ratio. The size of these specimens causes the cost of testing to be high and few labs have capacity for such specimens. The values in Table 4 are subsequently used by designers as an alternative to such testing, and the use of these conservative values is becoming an obstacle for concrete masonry construction in Alberta. Here, we compare testing of concrete block prism specimens with finite element models to understand how the material failure is altered with variations in the test configuration.

TEST SUMMARY

56 concrete block masonry prism specimens were tested under compressive axial load according to Annex D, CSA-S304-2014. The prism specimens were constructed in running bond with Type S mortar for both hollow and grouted prisms. A coarse grout was used to fill the cells (commonly referred to as cores) of the grouted prisms. Seven (7) prism specimens were constructed for each of the four nominal concrete masonry unit strengths (10, 15, 20 and 30 MPa), as typically manufactured by Expocrete (the largest manufacturer of concrete block in Alberta) for each condition (hollow and grouted). Thus 28 hollow and 28 grouted prism specimens were constructed. In addition to testing the hollow and grouted masonry prism specimens, five (5) units of each nominal unit strength were tested according to a slightly modified method of CSA-A165.1-04 to establish the specified compressive strength of the block units.

Materials

Concrete block masonry units of actual size of 390 mm × 190 mm × 190 mm manufactured by Expocrete were used. According to CSA-A165.1-04, at least five masonry units shall be tested to determine the specified compressive strength of units used for building the prisms. When less than 10 units are tested the Coefficient of Variation (C.O.V.) shall be assumed to be the greater of the measured C.O.V. and 10%. If the C.O.V. of the test results exceeds 15%, at least 10 units shall be tested. Type S mortar was used to construct the prisms. The mortar was mixed by combining Portland cement, lime, sand and water according to CSA-A179-2014, see Table 1. The grout was mixed according to proportion specification of CSA-A179-2014, see Table 2.

Table 1: Mortar Mixed According to Volume Proportion Specifications of CSA-A179-2014

Mortar type	Portland cement	Hydrated lime or lime putty	Aggregate measured in damp, loose state
S	1	½	3-½

Table 2: Grout Mixed According to Volume Proportion Specification of CSA-A179-2014

Grout type	Portland cement	Hydrated lime or lime putty	Aggregate measured in damp, loose state	
			Fine aggregate (sand)	Coarse aggregate
Coarse	1	0 to 1/10	2-1/4 to 3 times the sum of the cementitious material	1 to 2 times the sum of the cementitious material

Compression testing

Concrete blocks with nominal strengths of 10, 15, 20 and 30 MPa were used to construct the masonry prisms. The specifications for the prism construction are shown in Table 3. Seven grouted and seven hollow prisms were constructed for each of the nominal compressive strengths, see Figure 1. Mortar cubes and grout cylinders were also cast to determine their respective compressive strengths. The prisms were sealed and covered using polyethylene sheets for the first 7 days after construction, the sheets were then removed for curing up 21 days at which point the prisms were transported for 28 day testing.

Figure 1: Constructed Hollow and Grouted Prisms

Table 3: Material Strengths

Nominal Unit Strength [MPa]	Average Unit Strength [MPa]	Mortar Strength [MPa]	Grout Strength [MPa]
10	9.0	17.4	32.9
15	22.8	19.0	25.6
20	19.7	19.0	22.9
30	40.1	31.6	27.2

The grouted prisms were capped with Hydrostone^{TM} high-strength plaster for testing. The plaster was leveled to provide uniform contact with the testing machine platen. Hollow prisms were face shell loaded using 7/8" thick, 10 pound fibre board as per CSA-S304-2014 to achieve full contact between the platen of the test machine and the face shells of the concrete block units. The prisms were tested under concentric compression normal to the bed joint.

CSA-S304-2014

A summary of corrected grouted and hollow prism strengths is given in Table 4. It is evident that the strengths for both the hollow and grouted masonry prisms were much higher than the strengths interpolated from those in Table 4 of CSA-S304-2014. CSA-S304-2014 correction factors are given in Table 5.

Table 4: Corrected Prism Compressive Strength vs. Expocrete Concrete Block Strength

Specified Unit Strength (as per Annex C.2.2. in S304-14, from the data in Table 3) [MPa]	Grouted Concrete Block f 'm [MPa]		Hollow Concrete Block f 'm [MPa]	
	Table 4	Testing	Table 4	Testing
7.5	3.8	8.2	4.9	6.3
16.5	8.2	10.8	10.8	12.4
19.1	9.6	15.3	12.4	16.5
32.1	14.4	19.9	18.6	26.7

Table 5: Correction Factors, Table D.1 of CSA S304-2014

Height-to-Thickness Ratio	Correction Factor
2	0.85
3	0.90
4	0.95
5 to 10	1.00

FINITE ELEMENT MODELLING

Finite element modelling (FEM) was conducted using the micro-modelling approach to evaluate the failure and the subsequent correction factors applied when testing prisms between two and five units high. FEM of masonry structures is categorized as either macro or micro-modelling [2]. Macro-modelling can be utilized for structures with known macro properties, usually with the assumption that the components within the structure are fully bonded. Micro-modelling can be used when information is available for the constituent materials but the macro properties are unknown, making it suitable for the given problem. An accurate micro-model should include all the basic types of failure mechanisms that characterize masonry, such as cracking of the joints, sliding along the bed or head joints, tensile and diagonal cracking of the units, masonry crushing, [3]. Details of the model properties are outlined in the following sections.

Materials

Steel platens were represented with linear elastic material properties (E = 200 GPa, ν = 0.3) as they are not expected to exceed this range. Nonlinear materials properties were applied to the concrete units, mortar, and grout using the concrete damage plasticity (CDP) model in

Abaqus/Standard and Abaqus/Explicit which is based on work by Lubliner et al. [4]. Plasticity theory is used to approximate the behaviour of concrete and other similar materials which do not yield in reality. The assumption is that scalar damage occurs and is designed for applications in which the concrete is subjected to arbitrary loading conditions, including cyclic loading. The model takes into consideration the degradation of the elastic stiffness induced by plastic straining both in tension and compression. The yield function for the CDP model is defined in terms of effective stress and the corresponding stress invariant. Non-associated plastic flow is assumed using the Drucker-Prager hyperbolic function. Tension and compression are defined by separate hardening rules. For the following models, stress strain data were used to define both the compression and tensile behaviour. Based on testing of the constituent materials the material properties listed in Table 3 were used for the prism assemblies. Without more detailed testing data approximations were made to represent the material behaviour. For each of the three materials the modulus of elasticity was calculated using the equation for masonry [5] which is related to the component's compressive strength, f_c'.

$$E = 850 f_c' \tag{1}$$

The tensile strength of each material was calculated as

$$f_t' = 0.1 f_c' \tag{2}$$

Compressive stress strain relationships were obtained using the Loov equation [6]

$$\sigma_c = f_c' \left(\frac{\left(1 + B + \frac{1}{n-1}\right)\left(\frac{\varepsilon_c}{\varepsilon_o}\right)}{1 + B\left(\frac{\varepsilon_c}{\varepsilon_o}\right) + \frac{1}{n-1}\left(\frac{\varepsilon_c}{\varepsilon_o}\right)^n} \right) \tag{3}$$

Where ε_o is the strain at maximum compressive strength and ε_c is the strain at any compressive stress, σ_c. In equation [3] the two constants n and B can be chosen so that the curve can match the elastic modulus calculated previously up to 33% of the compressive strength. The maximum compressive stress occurs at a strain of 0.002 [5]. Values for 20 MPa prism materials are given in Table 6.

Compressive behaviour was used from five of the six critical points [7] on the stress-strain curve $0.33f_c'$, $0.75f_c'$, $0.9f_c'$, f_c', $0.5f_c'$, and $0.2f_c'$. Tension behaviour was assumed to be linear until f_t was reached, then at a ε_t the stress decreases to $0.6f_t$. The stress strain curve then decreases linearly to zero at $6\varepsilon_t$. However, due to numerical limitations the stress at $6\varepsilon_t$ was increased to $0.001f_t$ which is the minimum value permissible in the software [8]. An example of the critical points on the true stress strain curve is shown in Figure 2 for the 20 MPa block material.

Table 6: Material Parameters 20 MPa Prism

	f'_c [MPa]	f'_t [MPa]	E [GPa]	ν	B	n	$.33f'_c$ [MPa]	ε_c at $.33f'_c$ E-4
Block	19.72	1.97	16.76	0.19	0.031	2.43	6.51	3.88
Mortar	19.00	1.90	16.15	0.10	0.031	2.43	6.27	3.88
Grout	22.90	2.29	19.47	0.20	0.031	2.43	7.56	3.88

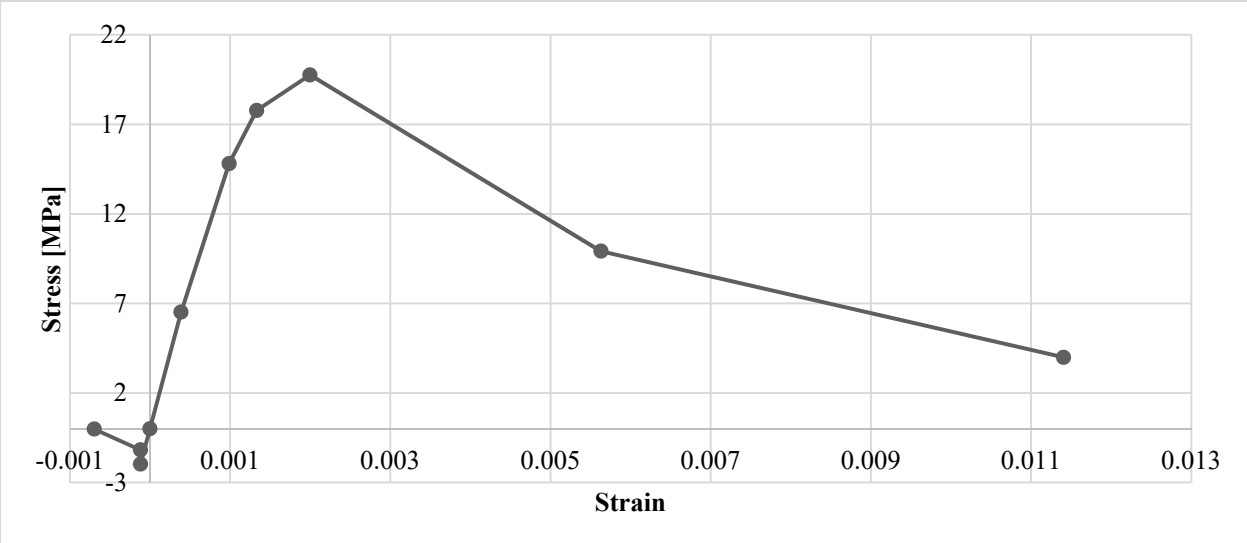

Figure 2: Stress – Strain Behaviour for Nominal 20 MPa Block

The concrete damage plasticity parameters were based on those recommended in the Abaqus documentation [8] and the values shown in Table 7 were consistent for all materials.

Table 7: Concrete Damage Plasticity Definition

ψ	e	f_{b0}/f_{c0}	K	Viscosity parameter
32	0.1	1.16	0.667	0.001

Geometry

Individual units and prism tests were modeled. Standard parts were established for units, grout, mortar, and steel and repeated in the assembly. Like materials were merged within the assembly when in contact. The geometry was based on nominal 200 mm concrete units with an actual size of 390 mm x 190 mm x 190 mm. To facilitate meshing rounded corners were not used. The geometry was otherwise accurately represented, accounting for the taper of the blocks and matching the grout to this profile. The standard unit geometry is shown in Figure 3 as well as a two high prism where the colours indicate use of different materials.

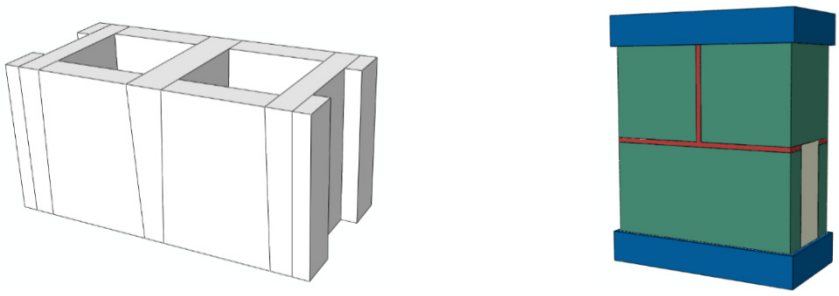

Figure 3: Concrete Unit Geometry and 2 Course (390 mm) Prism Test Assembly

Boundary Conditions

The effects of platen restraint are known to influence the results of compression testing. To examine these effects the individual units were loaded using varied end conditions to understand the effect on maximum compressive load. These variations are summarized in Table 8. Model B1 full constrains the horizontal displacements at the platen locations by setting the displacement to zero, while model B2 represents the other extreme, where these displacements are left as free and there is no interaction at the boundary. Models B3 – B5 include a steel platen through which the load is applied and the base restrained. The frictional interaction with this surface is varied from 0.3 to 0.7. In models B7 and B8 an additional part is included between the steel platen and the concrete block to represent fibreboard capping. The elastic modulus is consistent between the two models and the Poisson's ratio is varied from being equal to the steel value of 0.3 to the maximum value that can be entered of 0.495.

Table 8: Models for Boundary Condition Comparison

Model	Boundary Description
B1	U1 = U2 = 0
B2	U1 = U2 = free
B3	Friction 0.3
B4	Friction 0.5
B5	Friction 0.7
B7	Fibreboard E=4000 MPa ν=0.3
B8	Fibreboard E=4000 MPa ν=0.495

From Figure 4 it is evident that the highest strength is found when the boundary is fully constrained from permitting displacements in the horizontal directions (B1), while the lowest strength is found when these displacements are free (B2). Frictional contact with the steel platen gives similar performance to constraining the boundary, and it can be seen that as the friction was increased from 0.3 (B3) to 0.7 (B5) the failure load increased. However the effect of increasing the coefficient of friction is minor. When fibreboard is included (B7 and B8), increasing the Poisson's ratio value reduces the failure load by increasing the horizontal displacements at the boundaries.

Inclusion of fibreboard significantly increased the computational expense of the models. The prism samples were loaded through steel platens in frictional contact using a coefficient of 0.5.

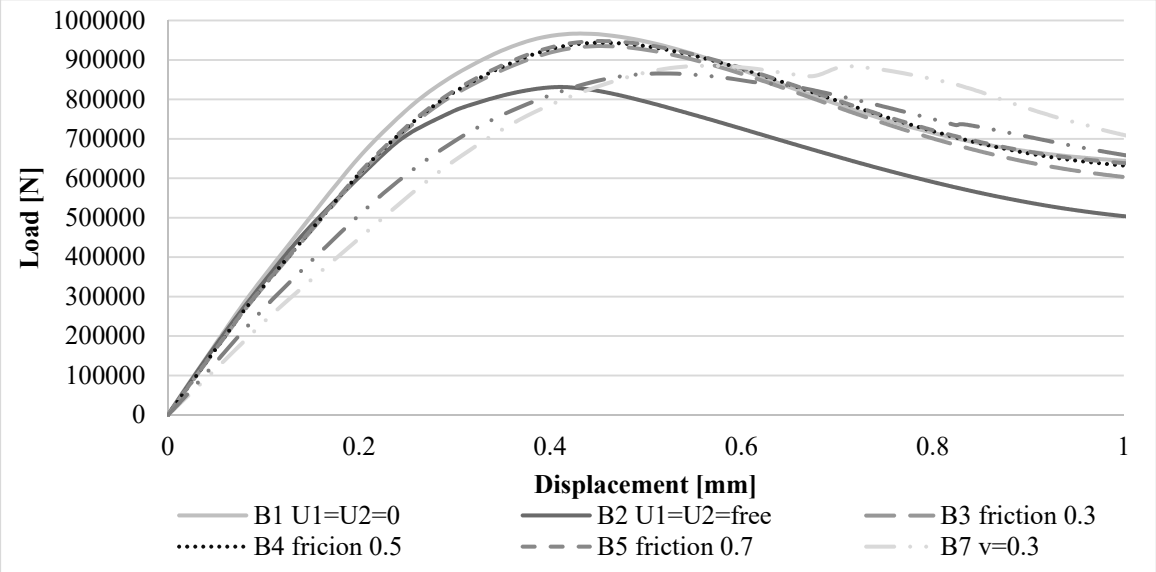

Figure 4: Load Displacement Curve 20 MPa Units Boundary Condition Study

Mesh Refinement

For the mesh refinement study Abaqus 8-node bilinear brick elements (C3D8) elements were used. The mesh density was varied by assigning a global element size. However, geometric variations caused some elements to deviate from this size. The mesh refinement study on the grouted prism assembly gave convergence of the solution with an average element size of 10 mm (Table 8).

Table 9: Mesh Refinement Study

Mesh	Avg. El. Size [mm]	No. Elements	No. Nodes	U3 at P_{max} [mm]
MR1	20	6998	11003	0.8125
MR2	10	43818	57016	0.8696
MR3	7	118251	143366	0.8696

Analysis Procedure

Contact and plasticity are both known to cause convergence issues which can be resolved with suitable numerical strategies, with selection of the strategy being related to the integration scheme which can be implicit or explicit within Abaqus. By enforcing equilibrium at each step of the analysis the implicit scheme used with Abaqus Standard is known to be reliable, while for the explicit scheme the issue of convergence is eliminated at the expense of some solution accuracy. Within the Abaqus Standard framework, the large displacement formulation and numerical stabilization would be required. In contrast, in the Abaqus Explicit mass scaling, time step, material density and average element size can be adjusted to accelerate convergence. It was possible to obtain convergence within the Standard integration scheme when the grouted parts

were assessed. Subsequently the ratio of viscous damping and total strain energy was checked, and convergence of the results was confirmed as the dissipated energy fraction was reduced.

Contact

The bond between the unit and the mortar can often be the weakest link; it is controlled by the unit-mortar interface and can exhibit tensile (mode I) and shear (mode II) failure [9]. Comparison of models with the conditions of full bonding between parts and frictional contact was completed to evaluate the need to include an intermediate level of cohesion between the parts. The load displacement curves for these models were plotted finding an increase in peak load of 5% when full bonding is considered between the parts. Subsequent modelling was conducted with the fully bonded prism to reduce computational expense of the analysis.

FEM RESULTS

Load displacement curves were plotted to compare 2 – 5 course (390 mm – 990 mm) test prisms for each unit strength. A typical graph is shown in Figure 5 for nominal 20 MPa grouted units. Figure 6 shows the plastic strain at peak load for each prism. The location of the head joints for units placed in running bond impacts the stress distribution, as does the asymmetry of the units due to tapering of the face shells. Platen confinement causes high strains at the corners of the 2 course prism. As expected, this confinement is reduced with increasing aspect ratio. In Table 10 the f'_m values are used to calculate correction factors. For unit strengths of 15 MPa and above the correction factors are found to be consistent with those established in Table D.1 of CSA-S304-2014, (Table 5). The high strength of grout used in combination with the low strength (10 MPa) units produced results inconsistent with the other models. When the 2 and 5 course models were analyzed using a 10 MPa grout the correction factor was found to be 0.86, which again is consistent with CSA- S304 Table D.1 and the other results.

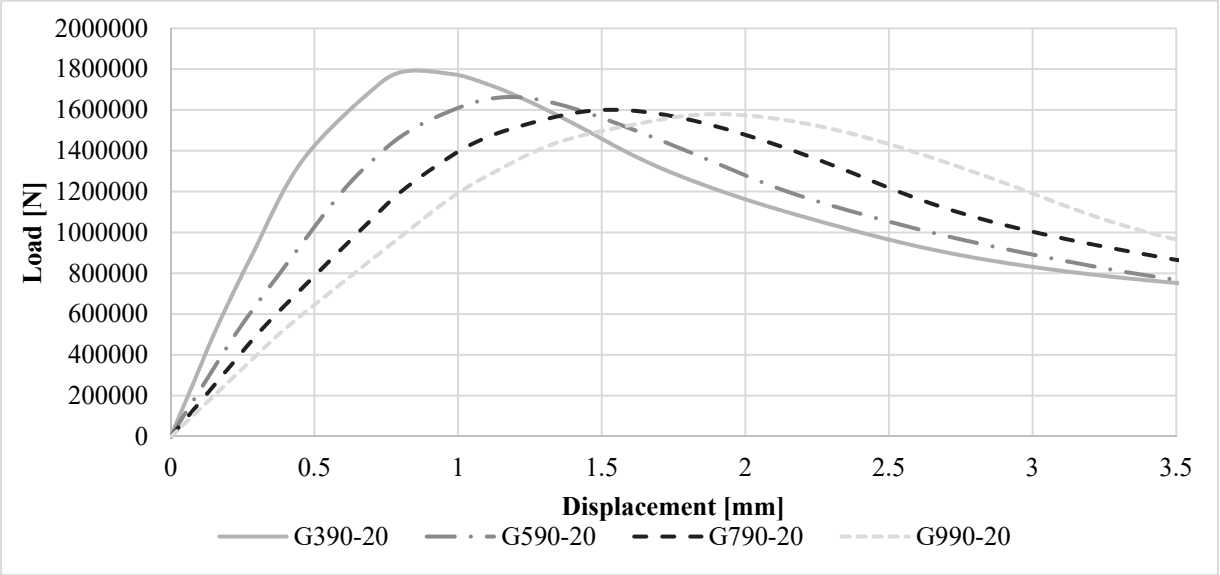

Figure 5: Nominal 20 MPa Load Displacement Curve

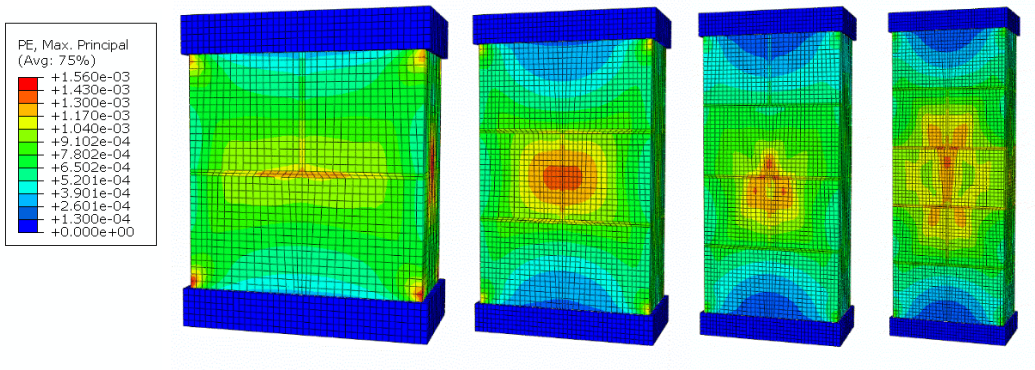

Figure 6: Comparison of plastic strain at P_{max} for grouted models 2-5 Courses High

Table 10: Peak Load and Compressive Strength Compared to the Five Unit High Model

Nominal Strength [MPa]	Prism Height [mm]	P_{rmax} [kN]	f'_m [MPa]	Correction Factor
10	390	1677	22.6	0.66
	590	1410	19.0	0.87
	790	1320	17.8	0.95
	990	1253	16.9	1.00
15	390	2035	27.5	0.86
	590	1883	25.4	0.95
	790	1808	24.4	0.99
	990	1786	24.1	1.00
20	390	1791	24.2	0.87
	590	1663	22.5	0.95
	790	1600	21.6	0.99
	990	1579	21.3	1.00
30	390	2824	38.1	0.82
	590	2628	35.5	0.90
	790	2460	33.2	0.97
	990	2390	32.3	1.00

CONCLUSIONS

Numerical models were developed for concrete units and testing prisms using simplified assumptions for the constituent materials. Inclusion of contact between parts was shown to have a minor effect on the results for this loading condition, and was subsequently omitted to reduce computation expense. Comparison of boundary condition showed full restraint of the horizontal constraints to overestimate the peak load when compared to frictional contact, while inclusion of fibreboard was shown to reduce the peak load. Frictional contact was used to represent the plaster to steel platen contact, while the frictional coefficient (varied between 0.3 and 0.7) had little impact on the load displacement behaviour. Refinement of the grout and mortar models based on better data should improve the results for the masonry assembly. The correction factors given in Table

D.1 of CSA-S304 were compared to those established through numerical modelling and were found to be consistent when unit and grout strengths were within a typical range. This result reinforces the hypothesis that the reduction in compressive strength with increasing prism height is primarily geometrical with the number of mortar joints in the sample having a lesser effect. This suggests that an accurate measure of the masonry material's compressive strength can be established with the testing of 2 high prisms or height to thickness ratios of approximately 2 (as is done in ASTM C1314 and concrete cylinder testing)

From the testing, the conservative strengths presented in Table 4 of CSA-S304 may be mitigated in Alberta by specification of proportion mixed Type S mortar that achieves a 28 day strength of 15 MPa or greater and proportion mixed Coarse Grout achieving a 28 day strength, corrected for non-absorptive cylinders, of 23 MPa or greater, and Expocrete concrete block masonry products. Table 4 was created by interpolating the compressive strength normal to the bed joint for the nominal block unit strengths from the test results and presents a more reasonable representation of the compressive strength of grouted and hollow masonry prisms. The overall results indicate that the compressive strength for grouted and hollow masonry can be increased within Alberta, and a similar program across Canada may allow for updating of the Table 4 values.

ACKNOWLEDGEMENTS

This research was funded through the Mitacs Accelerate program with the financial support of the Alberta Masonry Council. The authors also appreciate the contribution of material made available by Expocrete, and construction of the testing specimen by Pokar.

REFERENCES

[1] Maurenbrecher, A.P.H. (1986) "Compressive strength of hollow concrete blockwork." 4th Canadian Masonry Symposium. Fredericton, N.B.

[2] Lourenço, P.B. (1996). "Computational strategies for masonry structures." Delft Technical University" .

[3] Lourenço, P.B., Rots, J.G., and Blaauwendraad J. (1989). "Two approaches for the analysis of masonry structures: micro and macro-modelling." HERON, 40(4), 313-340.

[4] Lubliner, J., Oliver, J., Oller, S., Onate, E. (1989) "A Plastic-Damage Model for Concrete." International Journal of Solids and Structures, 25(3), 299-326.

[5] Drysdale, R. G. and Hamid, A. A. (2005). *Masonry Structures Behaviour and Design*, Canada Masonry Design Centre, Mississauga, ON, Canada.

[6] Loov, R.E. (1991) "A General Stress-Strain Curve for Concrete—Implications for High Strength Concrete Columns." *Proc., Annual Conference of the Canadian Society for Civil Engineering*. Vancouver, British Columbia, Canada.

[7] Kaushik, H.B., Rai, D.C., and Jain, S.K. (2007) "Stress-strain characteristics of clay brick masonry under uniaxial compression." Materials in Civil Engineering, 19(9), 728-739.

[8] Dassault Systems (2016) *ABAQUS 6.12 Documentation*. Providence, RI, USA.

[9] Lourenco, P.B. (2002) "Computations on historic masonry structures." Progress in Structural Engineering and Materials, 4(3), 301-319.